International Journal of Mass Spectrometry 276 (2008) 49–55

Contents lists available at ScienceDirect

International Journal of Mass Spectrometry

journal homepage: www.elsevier.com/locate/ijms

# Determination of branching ratios for the reactions of $H_3O^+$ with ethylbenzenes as a function of relative kinetic energy

Sohiko Kameyama [a,b], Satoshi Inomata [c,*], Hiroshi Tanimoto [b]

[a] Japan Society for the Promotion of Science, 8 Ichibancho, Chiyoda-ku, Tokyo 102–8472, Japan
[b] Asian Environment Research Group, National Institute for Environmental Studies, 16–2 Onogawa, Tsukuba, Ibaraki 305–8506, Japan
[c] Atmospheric Environment Division, National Institute for Environmental Studies, 16–2 Onogawa, Tsukuba, Ibaraki 305–8506, Japan

ARTICLE INFO

*Article history:*
Received 13 June 2008
Received in revised form 8 July 2008
Accepted 8 July 2008
Available online 16 July 2008

*Keywords:*
$H_3O^+$ + ethylbenzene reaction
Ethylbenzenium ion
Deuterium labeling
Hydrogen atom migration
PTR-MS

ABSTRACT

The proton-transfer reactions of $H_3O^+$ with ethylbenzene and deuterium-labeled ethylbenzenes were systematically investigated by means of proton-transfer reaction mass spectrometry. The branching ratios for the formation of protonated ethylbenzenes and for fragmentation reactions involving elimination of ethylene from the protonated molecules, accompanied by hydrogen migration from the α position or the β position of the ethyl group, were determined as a function of the mean relative center-of-mass kinetic energies of the reactants ($K_{cm}$). The branching ratio for the intact protonated molecule decreased with increasing relative kinetic energy: the branching ratio decreased from 0.87 at $K_{cm}$ = 0.19 eV to 0.05 at $K_{cm}$ = 0.36 eV, and in turn the ratio for ethylene elimination increased from 0.13 to 0.95. The branching ratios determined for partially deuterium-labeled ethylbenzenes were consistent with one another as well as with the ratios for unlabeled ethylbenzene. The fraction of H migration from the α position increased with increasing $K_{cm}$ (from 0.13 ± 0.01 at $K_{cm}$ = 0.19 eV to 0.24 ± 0.01 at $K_{cm}$ = 0.36 eV) and appeared to saturate at ~0.24 at $K_{cm}$ values above 0.28 eV.



## 1. Introduction

Interest in protonated alkylbenzenes developed with the introduction of chemical ionization mass spectrometry (CI-MS) [1–6]. Munson and Field [2] were the first to apply a methane CI technique to alkylbenzenes. In addition to the formation of protonated alkylbenzenes ($MH^+$) and cluster ions such as $M{\cdot}C_2H_5^+$ and $M{\cdot}C_3H_5^+$ ions, Munson and Field observed major fragments arising from the loss of H or alkyl groups from M, from olefin displacement by $H^+$ or $C_2H_5^+$, and, for larger alkyl substituents, from formation of alkyl ions. Hermann and Harrison [3] investigated the dependence of the fragmentation pattern—that is, the competition between olefin elimination (Eq. (1)) and alkyl ion formation (Eq. (2))—on the relative heats of reaction for $C_8$–$C_{11}$ alkylbenzenes by comparing the mass spectra obtained by means of $H_2$, $N_2/H_2$, $CO_2/H_2$, $N_2O/H_2$, and $CO/H_2$ CI-MS:

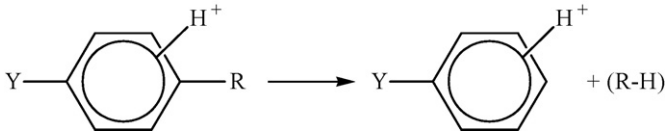


(1)

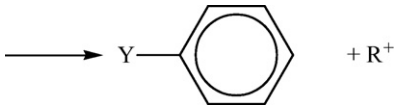


(2)

They found that for propylbenzenes and *n*-butylbenzene, olefin elimination (Eq. (1)) increases relative to alkyl ion formation (Eq. (2)) with decreasing protonation exothermicity. They proposed a fragmentation mechanism involving the formation of an incipient alkyl ion solvated by the neutral arene moiety, followed by isomerization to a proton-bound alkene–arene pair, which eventually decomposes by elimination of either the alkene or the arene fragment.

In the olefin elimination reaction (Eq. (1)), a hydrogen atom migrates from the alkyl group to the ring. Isotope-labeling studies are useful for elucidating mass spectrometric fragmentation

* Corresponding author. Tel.: +81 29 850 2403; fax: +81 29 850 2579.
*E-mail addresses:* kameyama.sohiko@nies.go.jp (S. Kameyama), ino@nies.go.jp (S. Inomata), tanimoto@nies.go.jp (H. Tanimoto).

1387-3806/$ – see front matter © 2008 Elsevier B.V. All rights reserved.
doi:10.1016/j.ijms.2008.07.002

mechanisms, and CI-MS studies involving deuterium labeling of the side chain have been performed for primary alkylbenzenes [7–10]. $H_2$, $D_2$, $CH_4$, and $CD_4$ CI studies of ethyl- and *n*-propylbenzenium ions by Leung and Harrison [7] showed that the migrating hydrogen atoms originate from all positions of the side chain for both compounds but that the ω positions are slightly preferred as donor sites. Leung and Harrison's results also suggested that the fraction of H migration from the α position depends slightly on the relative heats of reaction in the case of ethylbenzene:

$$XH^+ + C_6H_5C_2H_5 \rightarrow (C_6H_5C_2H_5{\cdot}H^+ + X) \rightarrow C_6H_7{}^+ + C_2H_4 + X \quad (3)$$

The heats of reaction ($\Delta H_r$) are −223 and −101 kJ mol$^{-1}$ for X = $H_2$ and $CH_4$, respectively [11]. Audier et al. [8] investigated the fraction of H migration by means of $H_2O$ CI, and their results were the same as those obtained by Leung and Harrison using $CH_4$ CI [7], even though $\Delta H_r$ for X = $H_2O$ is +46 kJ mol$^{-1}$ [11]. The similarity between the results by $CH_4$ CI and $H_2O$ CI is thought to be coincidental [6].

In the present study, we systematically investigated the reactions of $H_3O^+$ with ethylbenzene and deuterium-labeled ethylbenzenes to determine the dependence of the branching ratios between the formation of protonated ethylbenzenes and the fragmentation reactions on the relative kinetic energies of the reactants, since the isotope labeling studies were performed only at discrete energy levels even for the ethylbenzenium ion, which is a relatively simple alkylbenzenium ion. In addition to the branching ratios for the formation of the protonated molecules and the fragments, the branching ratios for H atom migration from the α and β positions of the ethylbenzenium ion in the fragmentation reactions were determined as a function of the relative kinetic energies by means of deuterium labeling of the ethyl group of ethylbenzene. These data should be useful for elucidating the mechanism of ethylbenzenium ion fragmentation, as well as for determining the energies of intermediates and reaction barriers [9,12]. Note that alkyl ion ($C_2H_5{}^+$) formation has a much higher heat of reaction ($\Delta H_r$ = + 116 kJ mol$^{-1}$ [11]) relative to that of the olefin elimination channel ($\Delta H_r$ = +46 kJ mol$^{-1}$), so the olefin elimination channel is the predominant fragmentation reaction for the ethylbenzenium ion [3].

The relative kinetic energy resolved mass spectra for the $H_3O^+$ + ethylbenzene reaction were obtained by means of proton-transfer reaction mass spectrometry (PTR-MS). PTR-MS is widely used for detecting and quantifying trace volatile organic compounds (VOCs) in the gas phase [13–15]. The proton donor is $H_3O^+$, which is generated relatively cleanly and simply in the gas-phase discharge without any need for mass pre-selection. The proton-transfer reactions between $H_3O^+$ and VOCs take place in a drift tube, where a homogeneous electric field of strength *E* is established to suppress the formation of hydronium ion–water clusters, such as $H_3O^+{\cdot}H_2O$. The relative kinetic energies of the reactants are controlled by variation of *E*.

## 2. Experimental

A commercially available PTR-MS instrument was used (Ionicon Analytik). The PTR-MS instrument, which has been described in detail elsewhere [13–16], consists of a discharge ion source to produce the $H_3O^+$ ions; a drift tube, in which the proton-transfer reactions between $H_3O^+$ and VOCs take place; and a quadrupole mass spectrometer (QMS) for the detection of reagent and product ions.

In a hollow cathode discharge ion source, $H_3O^+$ ions were produced from a pure water vapor flow of 7.8 sccm. The sample air was introduced into the drift tube at a flow rate of approximately 22 sccm; the drift tube pressure was held at 2.1 mbar. Most of the water vapors in the ion source were removed by a pump, but a small fraction of the water escaped into the drift tube. The water vapor concentrations in the drift tube was expected to be ∼10 mmol/mol [16]. The sampling inlet and drift tube were held at 105 °C. The drift tube (9.2 cm long) consisted of stainless steel ring electrodes, separated by Teflon rings for electrical isolation. The ring electrodes were connected to a resistor network, which divided the overall drift voltage ($U_{drift}$) into a homogeneously increasing voltage and established a homogeneous electric field inside the drift tube. The electric field was applied along the drift tube to avoid substantial formation of cluster ions, $H_3O^+{\cdot}(H_2O)_n$, *n* = 1, 2,. . . [17]:

$$H_3O^+ + H_2O \leftrightarrow H_3O^+{\cdot}H_2O \quad (4)$$

$$H_3O^+{\cdot}(H_2O)_n + H_2O \leftrightarrow H_3O^+{\cdot}(H_2O)_{n+1} \quad (5)$$

In the drift tube, trace gases such as VOCs in the sample air were ionized by proton-transfer reactions. A fraction of the reagent ion, $H_3O^+$, and the product ions was extracted through a small orifice into the QMS. The ions were detected by a secondary electron multiplier operated in the ion pulse counting mode. The mass dependence of the transmission efficiency of the QMS was calibrated by the manufacturer.

Ethylbenzene vapor was prepared by injecting a liquid sample into a 5-l Pyrex glass vessel [18], and mass spectra were obtained at six values of *E*/*N* (108, 119, 130, 140, 151, and 162 Td; 1 Td = $10^{-17}$ cm$^2$ V molecule$^{-1}$), where *E* is the electric field strength (V cm$^{-1}$) and *N* is the buffer gas number density (molecule cm$^{-3}$). A small amount of each sample (0.1 μl) was injected into the vessel and diluted with air from a zero-air supply (Model 111, Thermo Environmental Instruments Inc.), resulting in a sample mixture of approximately 2 parts per million by volume (ppmv). Data were recorded using the PTR-MS instrument's scan mode from *m*/*z* 21 to 125 with 0.5 s Da$^{-1}$ and were averaged for five mass spectra at each *E*/*N* ratio.

The count rate of the reagent ion, $H_3O^+$, calculated from the count rate at *m*/*z* 21 ($H_3{}^{18}O^+$) multiplied by 500, was in the range (4–6) × $10^6$ cps. The ratios of the ion intensity of $H_3O^+{\cdot}H_2O$ (*m*/*z* 37) to that of $H_3O^+$ were 0.03 at *E*/*N* = 108 Td and 0.0004 at *E*/*N* = 162 Td; that is, the intensity ratio strongly depended on the *E*/*N* ratio. The ratio of the ion intensity of $O_2{}^+$ (*m*/*z* 32), which was probably generated by back diffusion of air from the drift tube to the ion source, to that of $H_3O^+$ was 0.03–0.05. The ion count rates of the product ions totaled (4–12) × $10^3$ normalized counts per second (ncps) normalized to an $H_3O^+$ intensity of $10^6$ cps, which is within the linear dynamic range of the PTR-MS instrument.

The stated purities of the chemicals used were as follows: ethylbenzene, >98.0% ($C_6H_5CH_2CH_3$; Wako Pure Chemicals); ethylbenzene-$d_{10}$, 99.0 at.% D ($C_6H_5CD_2CD_3$; Acros Organics); ethyl-β,β,β-$d_3$-benzene, 96.1 at.% D ($C_6H_5CH_2CD_3$; C/D/N Isotopes); ethyl-α,α-$d_2$-benzene, 99.1 at.% D ($C_6H_5CD_2CH_3$; C/D/N Isotopes); and ethyl-α,α-$d_2$-benzene-$d_5$, 99.3 at.% D ($C_6D_5CD_2CH_3$; C/D/N Isotopes).

## 3. Results and discussion

PTR mass spectra of ethylbenzenes obtained at *E*/*N* = 108 Td are shown in Fig. 1, and the ion intensities of the product ions are summarized in Table 1. In the spectra, ion signals at *m*/*z* 32 ($O_2{}^+$) and *m*/*z* 37 ($H_3O^+{\cdot}H_2O$) are masked because they were largely scattered by the subtraction of the background mass spectrum.

In the mass spectrum of $C_6H_5CH_2CH_3$ (Fig. 1a), the peak of the protonated $C_6H_5CH_2CH_3$ ion (*m*/*z* 107) was the most intense. The peaks at *m*/*z* 79, 91, and 106, were assigned to $C_6H_7{}^+$, $C_7H_7{}^+$, and $C_6H_5CH_2CH_3{}^+$, respectively. The relative intensity of the signal at *m*/*z* 79 to that at *m*/*z* 107 was 0.15, whereas the relative intensities

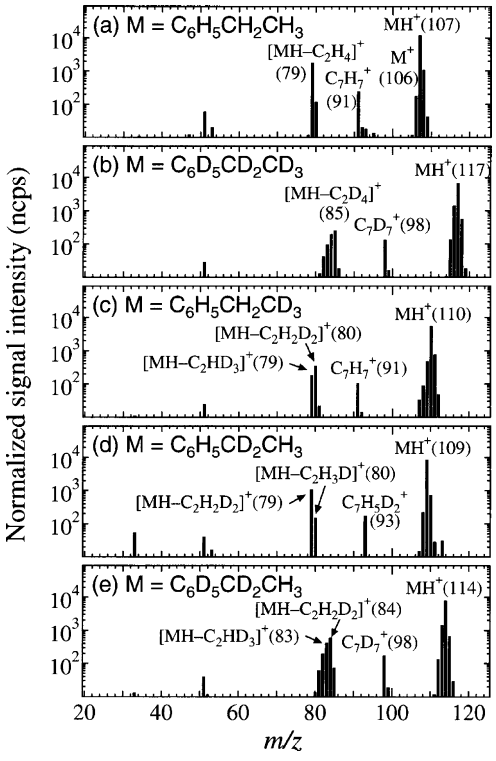


**Fig. 1.** PTR mass spectra for (a) $C_6H_5CH_2CH_3$, (b) $C_6D_5CD_2CD_3$, (c) $C_6H_5CH_2CD_3$, (d) $C_6H_5CD_2CH_3$, and (e) $C_6D_5CD_2CH_3$ at $E/N$ = 108 Td. Signal intensities are normalized to an $H_3O^+$ intensity of $10^6$ cps. From each mass spectrum, a background mass spectrum without ethylbenzene was subtracted. Values in parentheses show $m/z$.

for the signals at $m/z$ 91 and 106 were only 0.02 and 0.01, respectively. The $C_6H_7^+$ ion was formed by elimination of ethylene from protonated ethylbenzene (i.e., $[MH-C_2H_4]^+$):

$$C_6H_5CH_2CH_3 + H_3O^+ \rightarrow C_6H_5CH_2CH_3{\cdot}H^+ + H_2O$$
$$\Delta H_r = -97\ \text{kJ mol}^{-1} \quad (6a)$$

$$C_6H_5CH_2CH_3 + H_3O^+ \rightarrow C_6H_7^+ + C_2H_4 + H_2O$$
$$\Delta H_r = +46\ \text{kJ mol}^{-1} \quad (6b)$$

Both $C_7H_7^+$ and $C_6H_5CH_2CH_3^+$ were probably formed by the reaction of a small amount of $O_2^+$ in the drift tube with the ethylbenzene, as reported for a selected ion flow tube mass spectrometry (SIFT-MS) experiment [19]:

$$C_6H_5CH_2CH_3 + O_2^+ \rightarrow C_6H_5CH_2CH_3^+ + O_2$$
$$\Delta H_r = -318\ \text{kJ mol}^{-1} \quad (7a)$$

$$C_6H_5CH_2CH_3 + O_2^+ \rightarrow C_7H_7^+ + CH_3 + O_2$$
$$\Delta H_r = -147\ \text{kJ mol}^{-1} \quad (7b)$$

Indeed, the intensity of the $C_7H_7^+$ ion did not increase substantially with increasing $E/N$ (Table 2). In the SFIT-MS experiment [19], the formation of $C_6H_7^+$ during the reaction of $H_3O^+$ with ethylbenzene was not observed, because the reaction shown in Eq. (6b) is endothermic.

The very small peaks at $m/z$ 80, 92, and 108 in Fig. 1a were attributed to $^{13}C$ isotopologues of $C_6H_7^+$, $C_7H_7^+$, and $C_6H_5CH_2CH_3{\cdot}H^+$, respectively. The ratios of the ion count rates at $m/z$ 80, 92, and 108 to the rates at $m/z$ 79, 91, and 107 were $0.066 \pm 0.002$, $0.079 \pm 0.005$, and $0.088 \pm 0.005$, respectively. Error limits represent 95% confidence levels as determined by $t$-test. We obtained the values shown in Table 1 by subtracting the possible ion counts from the $^{13}C$ isotopologues using these ratios.

In the mass spectrum of $C_6D_5CD_2CD_3$ (Fig. 1b), like that of $C_6H_5CH_2CH_3$ (Fig. 1a), intense peaks for the protonated $C_6D_5CD_2CD_3$ ion and a fragment ion generated by elimination of $C_2D_4$ from protonated $C_6D_5CD_2CD_3$ were observed at $m/z$ 117 and 85, respectively, along with a peak for the byproduct ion $C_7D_7^+$ at $m/z$ 98. Noted that there was no signal at $m/z$ 86, which corresponds to the mass of $[MH-C_2HD_3]^+$ (Table 1); the absence of this signal suggests that the ethylene was eliminated only from the ethyl group of an ethylbenzene:

$$C_6D_5CD_2CD_3 + H_3O^+ \rightarrow C_6D_5CD_2CD_3{\cdot}H^+ + H_2O \quad (8a)$$
$$C_6D_5CD_2CD_3 + H_3O^+ \rightarrow C_6D_6H^+ + C_2D_4 + H_2O \quad (8b)$$

However, the ion intensity at $m/z$ 116 was higher than expected on the basis of the results observed for $C_6H_5CH_2CH_3$. In addition, the intensities of the ion signals at $m/z$ 84, 83, 82, and 81 were considerable (Table 1). Some H/D exchanges at the ring, the side chain, or both might have occurred with ambient water vapor in the drift tube:

$$C_8D_{10}{\cdot}H^+ + H_2O \rightarrow C_8H_2D_9^+ + HDO \quad (9)$$
$$C_6HD_6^+ + H_2O \rightarrow C_6H_2D_5^+ + HDO \quad (10)$$

In Table 1, the $C_8H_2D_9^+$ ion is denoted $[MH-1]^+$. Similarly, the $C_8H_3D_8^+$ ion is denoted $[MH-2]^+$. The H/D exchange

**Table 1**
Normalized signal intensities (ncps) of product ions in reactions of $H_3O^+$ with ethylbenzenes at $E/N$ = 108 Td[a]

| Ethylbenzene (M) | $MH^+$ | $M^+$<br>$M^+ + [MH-1]^+$ | –<br>$[MH-2]^+$ | $[MH-C_2H_4]^+$<br>$[M-CH_3]^+$ | $[MH-C_2H_3D]^+$<br>– | $[MH-C_2H_2D_2]^+$<br>– | $[MH-C_2HD_3]^+$<br>– | $[MH-C_2D_4]^+$<br>$[M-CD_3]^+$ |
|---|---|---|---|---|---|---|---|---|
| $C_6H_5CH_2CH_3$ | 11959 (107) | 177 (106) | – | 1764 (79) | – | – | – | – |
| | | – | – | 246 (91) | – | – | – | – |
| $C_6D_5CD_2CD_3$ | 6670 (117) | – | – | – | – | – | 1 (86) | 245 (85)[b] |
| | | 1399 (116) | 136 (115) | – | – | – | – | 133 (98) |
| $C_6H_5CH_2CD_3$ | 5516 (110) | – | – | – | – | 337 (80) | 182 (79) | – |
| | | 472 (109) | 88 (108) | – | – | – | – | 107 (91) |
| $C_6H_5CD_2CH_3$ | 8566 (109) | – | – | – | 81 (80) | 1097 (79) | – | – |
| | | 225 (108) | 15 (107) | 174 (93) | | – | – | – |
| $C_6D_5CD_2CH_3$ | 7802 (114) | – | – | – | 35 (85) | 573 (84)[c] | – | – |
| | | 1431 (113) | 132 (112) | 173 (98) | | – | – | – |

[a] Signal intensities were normalized to an $H_3O^+$ intensity of $10^6$ cps. Values in parentheses show $m/z$. Interference from $^{13}C$ isotopologues was subtracted (see text).
[b] Signal intensities were 190, 95, 42, and 13 ncps at $m/z$ 84, 83, 82, and 81, respectively.
[c] Signal intensities were 413, 197, 61, and 14 ncps at $m/z$ 83, 82, 81, and 80, respectively.

**Table 2**
Normalized signal intensities (ncps) of product ions in reactions of $H_3O^+$ with ethylbenzenes at $E/N$ = 162 Td[a]

| Ethylbenzene (M) | $MH^+$ | $M^+$<br>$M^+ + [MH-1]^+$ | –<br>$[MH-2]^+$ | $[MH-C_2H_4]^+$<br>$[M-CH_3]^+$ | $[MH-C_2H_3D]^+$<br>– | $[MH-C_2H_2D_2]^+$<br>– | $[MH-C_2HD_3]^+$<br>– | $[MH-C_2D_4]^+$<br>$[M-CD_3]^+$ |
|---|---|---|---|---|---|---|---|---|
| $C_6H_5CH_2CH_3$ | 387 (107) | 23 (106)<br>– | –<br>– | 7950 (79)<br>363 (91) | –<br>– | –<br>– | –<br>– | –<br>– |
| $C_6D_5CD_2CD_3$ | 340 (117) | –<br>41 (116) | –<br>6 (115) | –<br>– | –<br>– | –<br>– | 19 (86) | 3706 (85)[b]<br>238 (98) |
| $C_6H_5CH_2CD_3$ | 238 (110) | –<br>26 (109) | –<br>16 (108) | –<br>– | –<br>– | 2552 (80)<br>– | 1612 (79)<br>– | –<br>169 (91) |
| $C_6H_5CD_2CH_3$ | 325 (109) | –<br>19 (108) | –<br>7 (107) | –<br>254 (93) | 942 (80)<br>– | 5058 (79)<br>– | –<br>– | –<br>– |
| $C_6D_5CD_2CH_3$ | 325 (114) | –<br>30 (113) | –<br>4 (112) | –<br>242 (98) | 724 (85)<br>– | 4009 (84)[c]<br>– | –<br>– | –<br>– |

[a] Signal intensities were normalized to an $H_3O^+$ intensity of $10^6$ cps. Values in parentheses show $m/z$. Interference from $^{13}C$ isotopologues was subtracted (see text).
[b] Signal intensities were 1272, 261, 83, and 144 ncps at $m/z$ 84, 83, 82, and 81, respectively.
[c] Signal intensities were 1154, 207, 142, and 105 ncps at $m/z$ 83, 82, 81, and 80, respectively.

seems to have been substantial for benzenium-type ions rather than for ethylbenzenium-type ions, because the fractions for H/D exchange were estimated to be 0.18 (=(1399 + 136 − 119)/(6670 + 1399 + 136 − 119)) for ethylbenzenium-type ions and 0.58 (=(190 + 95 + 41 + 13)/(245 + 190 + 95 + 42 + 13)) for benzenium-type ions, respectively. In this estimation, the ion signals for $M^+$ calculated by using an $M^+/MH^+$ ratio obtained for $C_6H_5CH_2CH_3$ were subtracted. Because the production of $H_2DO^+$ was not observed, the extent of an H/D exchange between $H_3O^+$ and ethylbenzene-$d_{10}$ in reaction (11) is probably too small to be observed:

$$C_8D_{10} + H_3O^+ \rightarrow C_8HD_9 + H_2DO^+ \quad (11)$$

In the mass spectra of partially deuterium-labeled ethylbenzenes, we observed a peak for protonated ethylbenzene, denoted $MH^+$, and peaks for two kinds of product ions produced by elimination of ethylene from protonated ethylbenzene (Fig. 1c–e), that is, $[MH-C_2HD_3]^+$ and $[MH-C_2H_2D_2]^+$ for $C_6H_5CH_2CD_3$, and $[MH-C_2H_3D]^+$ and $[MH-CH_2D_2]^+$ for $C_6H_5CD_2CH_3$ and $C_6D_5CD_2CH_3$, respectively.

$$C_6H_5CH_2CD_3 + H_3O^+ \rightarrow C_6H_5CH_2CD_3{\cdot}H^+ + H_2O \quad (12a)$$

$$C_6H_5CH_2CD_3 + H_3O^+ \rightarrow C_6H_7{}^+ + C_2HD_3 + H_2O \quad (12b_\alpha)$$

$$C_6H_5CH_2CD_3 + H_3O^+ \rightarrow C_6H_6D^+ + C_2H_2D_2 + H_2O \quad (12b_\beta)$$

$$C_6H_5CD_2CH_3 + H_3O^+ \rightarrow C_6H_5CD_2CH_3{\cdot}H^+ + H_2O \quad (13a)$$

$$C_6H_5CD_2CH_3 + H_3O^+ \rightarrow C_6H_6D^+ + C_2H_3D + H_2O \quad (13b_\alpha)$$

$$C_6H_5CD_2CH_3 + H_3O^+ \rightarrow C_6H_7{}^+ + C_2H_2D_2 + H_2O \quad (13b_\beta)$$

$$C_6D_5CD_2CH_3 + H_3O^+ \rightarrow C_6D_5CD_2CH_3{\cdot}H^+ + H_2O \quad (14a)$$

$$C_6D_5CD_2CH_3 + H_3O^+ \rightarrow C_6D_6H^+ + C_2H_3D + H_2O \quad (14b_\alpha)$$

$$C_6D_5CD_2CH_3 + H_3O^+ \rightarrow C_6D_5H_2{}^+ + C_2H_2D_2 + H_2O \quad (14b_\beta)$$

Our results indicate that H atom migration from both the α and β positions of the side chain occurred in the ethylene elimination reaction, as reported previously [7,8]. In the mass spectrum of $C_6D_5CD_2CH_3$, the H/D exchange was substantial for both the benzenium-type ions and the ethylbenzenium-type ions, as was the case for $C_6D_5CD_2CD_3$; whereas H/D exchange seems to have been suppressed for $C_6H_5CH_2CD_3$ and $C_6H_5CD_2CH_3$. The fractions of H/D exchange for ethylbenzenium-type ions were 0.08, 0.01, and 0.16 for $C_6H_5CH_2CD_3$, $C_6H_5CD_2CH_3$, and $C_6D_5CD_2CH_3$, respectively, and these values likely depended on the number of deuterium atoms; the values also suggest that H/D exchange at the α position did not take place readily. The fraction of H/D exchange for benzenium-type ions was estimated to be 0.54 for $C_6D_5CD_2CH_3$, which suggests that the exchange reaction depended on the number of deuterium atoms in this case too.

Similar PTR mass spectra were also obtained at different $E/N$ ratios; the PTR mass spectra of ethylbenzenes obtained at $E/N$ = 162 Td are shown in Fig. 2, and the ion intensities of product ions are listed in Table 2. The relative intensities of the protonated molecules and the fragment ions changed; that is, the intensity of the $MH^+$ peak decreased with increasing $E/N$ ratio, whereas that of the [MH−ethylene]$^+$ peak increased. However, the same peaks were observed in both sets of spectra; no new product ions were observed. This result suggests that only two reaction channels (Eqs. (6a) and (6b)) should be considered in this relative

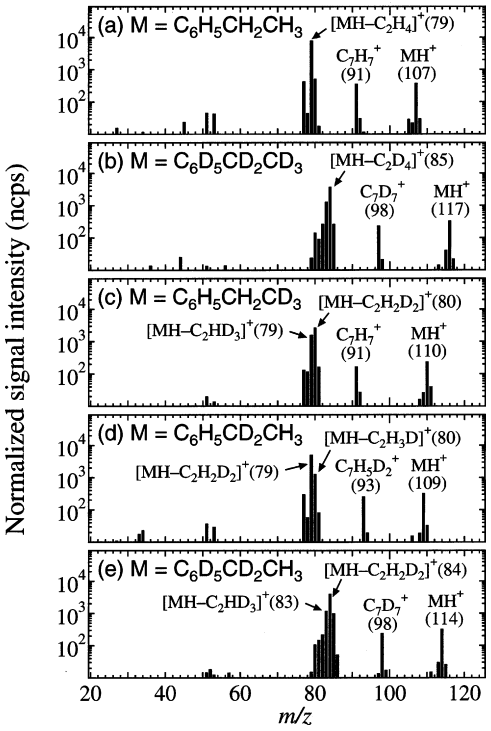


**Fig. 2.** PTR mass spectra for (a) $C_6H_5CH_2CH_3$, (b) $C_6D_5CD_2CD_3$, (c) $C_6H_5CH_2CD_3$, (d) $C_6H_5CD_2CH_3$, and (e) $C_6D_5CD_2CH_3$ at $E/N$ = 162 Td. Signal intensities are normalized to an $H_3O^+$ intensity of $10^6$ cps. From each mass spectrum, a background mass spectrum without ethylbenzene was subtracted. Values in parentheses show $m/z$.

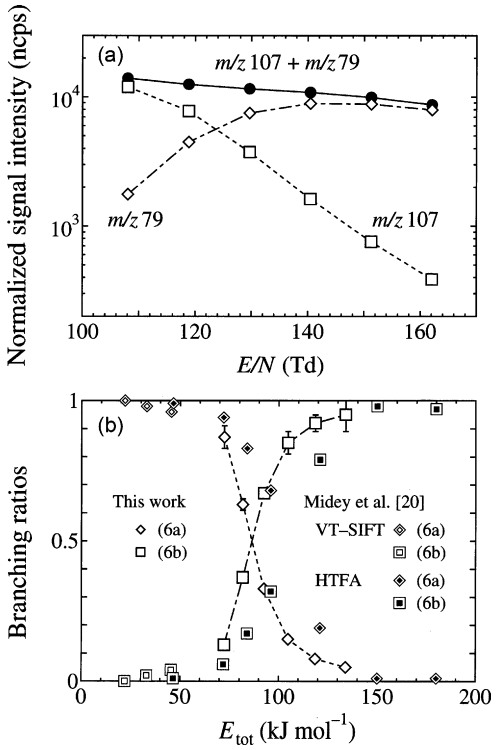


**Fig. 3.** (a) Dependence of ion count rates at $m/z$ 107 (open squares) and $m/z$ 79 (open diamonds) on $E/N$ ratio. The sums of ion count rates of $m/z$ 79 and 107 are shown as filled circles. (b) Dependence of the fraction between Eqs. (6a) and (6b) on the total average energy available for reaction, $E_{tot}$ (kJ mol$^{-1}$).

kinetic energy range. With regard to H/D exchange, the fractions for H/D exchange for benzenium ions were 0.32 for $C_6D_5CD_2CD_3$ and 0.29 for $C_6D_5CD_2CH_3$, and these values were lower than those at $E/N$ = 108 Td, which again indicates a dependence on the number of deuterium atoms.

Fig. 3a showed the dependence of the intensities of the peaks for protonated ethylbenzene ($MH^+$, $m/z$ 107) and $[MH-C_2H_4]^+$ ($C_6H_7^+$, $m/z$ 79) obtained from the reaction shown in Eq. (6) on the $E/N$ ratio. As mentioned above, the intensity of the $MH^+$ peak decreased substantially with increasing $E/N$, whereas that of $[MH-C_2H_4]^+$ increased. The total intensity of both ion signals decreased slightly. This decrease is because the estimated time of reaction in the drift tube decreased with increasing $E/N$, from 113 μs at 108 Td to 76 μs at 162 Td [16]. The total intensity correlated well with the estimated reaction time ($r^2$ = 0.986), suggesting that the rate constants for the reaction between $H_3O^+$ and ethylbenzene are constant at the whole $E/N$ ratios in the present study. This is consistent with results of the previous study using a variable temperature-selected ion flow tube (VT-SIFT) and a high-temperature flowing afterglow (HTFA) by Midey et al. [20] who reported that the $H_3O^+$ + ethylbenzene reaction rate constants are equal to the collision rate constants given by the Su-Chesnavich equation [21] at temperatures between 298 and 1000 K. Therefore, we concluded that the ratio of the ion intensities at $m/z$ 107 and 79 represented the branching ratios of the reaction channels shown in Eqs. (6a) and (6b). The branching ratios are shown in Table 3, along with the mean relative center-of-mass kinetic energy values ($K_{cm}$) [13,22]. A similar dependence of the fraction between Eqs. (6a) and (6b) on the kinetic energy has been observed in previous studies using other techniques, including VT-SIFT, HTFA [20], and high-pressure collisional activation [23].

In order to compare with the results from the VT-SIFT, and HTFA studies [20], the total average energy available for reaction, $E_{tot}$ (kJ mol$^{-1}$), was estimated by the following equations:

$$E_{tot} = KE(\text{ion}) + E_{rot}(\text{ion}) + E_{vib}(\text{ion}) + KE(\text{EB}) + E_{rot}(\text{EB}) + E_{vib}(\text{EB}) \quad (15)$$

where the KE (ion), $E_{rot}$ (ion), and $E_{vib}$ (ion) represent the average kinetic, rotational, and vibrational energies of the $H_3O^+$ ion, respectively, while the $KE$ (EB), $E_{rot}$ (EB), and $E_{vib}$ (EB) are those for ethylbenzene, respectively. The average kinetic energy and the average rotational energy in both the ionic and neutral reactants are each $3/2k_bT$, where $k_b$ is the Boltzmann constant. The average vibrational energies for the ionic and neutral reactants represent ensemble averages over Boltzmann distributions in the harmonic approximation. In the estimation of $KE$ (ion), $E_{rot}$ (ion), and $E_{vib}$ (ion), an effective kinetic temperature, $T_{eff}$, for an ion moving at $v_d$ calculated by $T_{eff} = T_{drift} + M_B v_d^2/(3k_b)$ was used [24], where $T_{drift}$ is the temperature of the drift tube and $M_B$ is the mass of the bath gas. On the other hand, $T_{drift}$ was used in the estimation of $KE$ (EB), $E_{rot}$ (EB) and $E_{vib}$ (EB). The ethylbenzene vibrational frequencies were calculated using Gaussian 98 for all normal modes with B3LYP/6-31G* [25] and were scaled by a factor of 0.9613 [26]. The vibrational frequencies for $H_3O^+$ were taken from the NIST-JANNAF thermochemical tables [27]. The calculated $E_{tot}$ was listed in Table 3. Fig. 3b

**Table 3**
Branching ratios in the $H_3O^+$ + ethylbenzene reaction[a]

| $E/N$ (Td) | 108 | 119 | 130 | 140 | 151 | 162 |
|---|---|---|---|---|---|---|
| $K_{cm}$ (eV)[b] | 0.19 | 0.22 | 0.25 | 0.28 | 0.32 | 0.36 |
| $E_{tot}$ (kJ mol$^{-1}$)[c] | 72 | 82 | 93 | 105 | 119 | 134 |
| $C_6H_5CH_2CH_3$ | | | | | | |
| Reaction (6a) | 0.87 ± 0.04 | 0.63 ± 0.02 | 0.33 ± 0.01 | 0.15 ± 0.01 | 0.08 ± 0.01 | 0.05 ± 0.01 |
| Reaction (6b) | 0.13 ± 0.01 | 0.37 ± 0.01 | 0.67 ± 0.02 | 0.85 ± 0.04 | 0.92 ± 0.03 | 0.95 ± 0.06 |
| $C_6H_5CH_2CD_3$ | | | | | | |
| Reaction (12a) | 0.88 ± 0.03 | 0.65 ± 0.03 | 0.34 ± 0.01 | 0.15 ± 0.01 | 0.07 ± 0.01 | 0.04 ± 0.01 |
| Reaction (12b$_\alpha$) | 0.02 ± 0.01 | 0.06 ± 0.01 | 0.14 ± 0.01 | 0.20 ± 0.01 | 0.23 ± 0.02 | 0.24 ± 0.02 |
| Reaction (12b$_\beta$)[d] | 0.10 ± 0.01 | 0.29 ± 0.02 | 0.52 ± 0.03 | 0.65 ± 0.02 | 0.70 ± 0.05 | 0.72 ± 0.03 |
| $C_6H_5CD_2CH_3$ | | | | | | |
| Reaction (13a) | 0.87 ± 0.03 | 0.63 ± 0.02 | 0.34 ± 0.01 | 0.15 ± 0.01 | 0.08 ± 0.01 | 0.05 ± 0.01 |
| Reaction (13b$_\alpha$)[d] | 0.02 ± 0.01 | 0.07 ± 0.01 | 0.14 ± 0.01 | 0.20 ± 0.01 | 0.22 ± 0.02 | 0.23 ± 0.02 |
| Reaction (13b$_\beta$) | 0.11 ± 0.01 | 0.30 ± 0.01 | 0.52 ± 0.02 | 0.65 ± 0.02 | 0.70 ± 0.03 | 0.72 ± 0.03 |
| $i$ | 1.70 ± 0.09 | 1.62 ± 0.06 | 1.62 ± 0.04 | 1.63 ± 0.04 | 1.60 ± 0.05 | 1.59 ± 0.05 |
| $\alpha_1$ | 0.13 ± 0.01 | 0.18 ± 0.01 | 0.21 ± 0.01 | 0.24 ± 0.01 | 0.24 ± 0.01 | 0.24 ± 0.01 |

[a] Error limits were calculated by propagation of errors of the ion counts and indicate precision only. The errors of the ion counts were derived from 95% confidence levels by $t$-test.
[b] The mean relative center-of-mass kinetic energy.
[c] The total average energy available for reaction.
[d] The isotope effect favoring H migration over D migration ($i$) was included in the derivation.

shows a plot of the fraction between Eqs. (6a) and (6b) against the $E_{tot}$, which is in moderately good agreement with the results of the VT-SIFT and HTFA by Midey et al. [20].

The fractions of reaction channels ($12b_\alpha$), ($12b_\beta$), ($13b_\alpha$), and ($13b_\beta$) as well as reaction channels (12a) and (13a) were determined from the results in reactions (12) and (13). According to Leung and Harrison [7], the ratio of H migration to D migration for $C_6H_5CD_2CH_3$ and $C_6H_5CH_2CD_3$ can be expressed as follows:

$$\alpha, \alpha - d_2 : \frac{\text{H migration}}{\text{D migration}} = \frac{(1-\alpha_1)\, i}{\alpha_1} \tag{16}$$

$$\beta, \beta, \beta - d_3 : \frac{\text{H migration}}{\text{D migration}} = \frac{\alpha_1\, i}{1-\alpha_1} \tag{17}$$

where $\alpha_1$ is the fraction of H migration from the $\alpha$ position of the ethyl group and $i$ is the isotope effect favoring H migration over D migration. Because substantial H/D exchange was observed for benzenium-type ions in the cases of $C_6D_5CD_2CD_3$ and $C_6D_5CD_2CH_3$, the influence of H/D exchange on benzenium-type ions must be taken in a consideration. In the reactions shown in Eqs. (12) and (13), two types of benzenium ions, $C_6H_7^+$ and $C_6H_6D^+$, were produced. If the H/D exchange occurred, it took place just once for the $C_6H_6D^+$ ion. The fraction of the "single" H/D exchange was estimated from the fractions for H/D exchange obtained for $C_6D_5CD_2CD_3$ and $C_6D_5CD_2CH_3$. For example, the ratio of the intensity of the product ions after the H/D exchange to the intensity of $C_6HD_6^+$ was 1.39 (=(190+95+42+13)/245), whereas the ratio of the intensity of the product ions after the H/D exchange to the intensity of $C_6H_2D_5^+$ was 1.20 (=(413+197+61+14)/573) at $E/N$ = 108 Td. A factor for the "single" H/D exchange is defined here as the average of 0.19 (=1.39 − 1.20), 0.23 (=1.39/6), and 0.24 (=1.20/5), that is, $f$ ($E/N$ = 108 Td) = 0.22 ± 0.06. This factor depended on the $E/N$ ratio, which was 0.15 ± 0.01 at 119 Td, 0.11 ± 0.02 at 130 Td, 0.09 ± 0.01 at 140 Td, 0.09 ± 0.01 at 151 Td, and 0.08 ± 0.01 at 162 Td. Error limits represent 95% confidence levels by $t$-test.

By using this factor, we corrected the ion signals for the $C_6H_7^+$ and $C_6H_6D^+$ ions as follows.

$$I^{corr}(C_6H_6D^+) = I(C_6H_6D^+) + f \times I(C_6H_6D^+) \tag{18}$$

$$I^{corr}(C_6H_7^+) = I(C_6H_7^+) - f \times I(C_6H_6D^+) \tag{19}$$

The obtained branching ratios for channels ($12b_\alpha$), ($12b_\beta$), ($13b_\alpha$), and ($13b_\beta$) as well as channels (12a) and (13a) are listed in Table 3, along with $\alpha_1$ and $i$ values. The ion counts for the protonated ethylbenzenes used in the calculations were the sums of those of $MH^+$, $[MH-1]^+$, and $[MH-2]^+$. As shown in Table 3, the branching ratios for channels (12a) and (13a) obtained for $C_6H_5CH_2CD_3$ and $C_6H_5CD_2CH_3$, respectively, were in good agreement with those obtained for $C_6H_5CH_2CH_3$, which suggests that the isotope effect favoring H migration over D migration ($i$) was correctly estimated, because this value was used for channel ($12b_\beta$) and channel ($13b_\alpha$). The fraction of H migration from the α position, $\alpha_1$, depended on the mean relative center-of-mass kinetic energy ($K_{cm}$). The $\alpha_1$ value increased when $K_{cm}$ was increased from 0.13 ± 0.01 to 0.24 ± 0.01 and was likely saturated at an $\alpha_1$ value of ~0.24 for $K_{cm}$ values above 0.28 eV. In contrast, the value of $i$ was likely independent of $K_{cm}$. The best representation for $i$ is just the average, 1.63 ± 0.04, where the indicated error limit represent the 95% confidence level by $t$-test.

Fig. 4 shows a plot of $i$ vs. $\alpha_1$; the data obtained in the present study are shown as filled circles with error limits, and data from previous studies [7,8] are also plotted. Our data overlapped with the data for $CH_4$, $CD_4$, and $H_2O$ CI, but the data for $H_2$ and $D_2$ CI gave higher $\alpha_1$ values and lower $i$ values. It is likely that the previous data obtained by $H_2$, $D_2$, $CH_4$, and $CD_4$ CI-MS [7] include some inconsistent results. For example, the ratio of channels (6b) to (6a) was reported to be 0.182 as determined by $CH_4$ CI, whereas the ratios of channels (12b) to (12a) and channels (13b) to (13a) were estimated to be 0.375 (=0.046 × 1.76 + 0.294) and 0.301 (=0.135 × 1.76 + 0.063), respectively. This inconsistency may have been caused by the problem of the linear dynamic range of the instrument and the interference of side reactions. The linear dynamic range of the instrument we used for the present study was guaranteed by the fact that the ratios of ion counts from the $^{13}C$ isotopologues (0.066 ± 0.002, 0.079 ± 0.005, and 0.088 ± 0.005 for $C_6$, $C_7$, and $C_8$ compounds, respectively) were consistent with the values calculated by multiplying 0.011 by the number of carbons. As for the interference of side reactions, the production of $O_2^+$ and $H_3O^+ \cdot H_2O$ ions was suppressed (the amount of these ions was less than a few percent of that of $H_3O^+$ ion), so side reactions could be considered negligible in the present study.

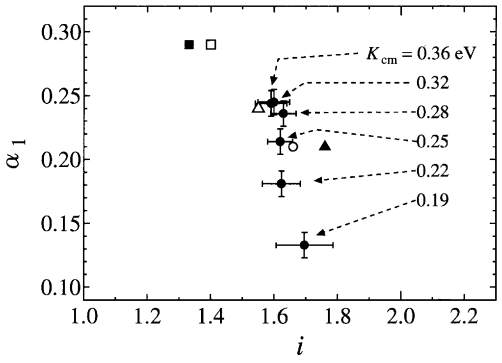


**Fig. 4.** Plot of $i$ (the isotope effect favoring H migration over D migration) vs. $\alpha_1$ (the fraction of H migration from the $\alpha$ position). PTR-MS (this work, filled circles); $H_2$ CI (filled square), $D_2$ CI (open square), $CH_4$ CI (filled triangle), $CD_4$ CI (open triangle) [7]; $H_2O$ CI (open circle) [8].

## 4. Conclusions

We systematically investigated the reactions of $H_3O^+$ with ethylbenzene and deuterium-labeled ethylbenzenes by PTR-MS to determine the dependence of the branching ratios between the formation of protonated ethylbenzenes and the fragmentation reactions resulting from elimination of ethylene from the protonated molecules accompanied by hydrogen migration at the α and β positions of the ethyl group on the relative kinetic energies ($K_{cm}$) of the reactants. The branching ratio for the intact protonated molecule decreased with increasing $E/N$ ratio (from 0.87 at $K_{cm}$ = 0.19 eV to 0.05 at $K_{cm}$ = 0.36 eV), whereas the ratio for fragmentation increased from 0.13 to 0.95. The results obtained for partially deuterium-labeled ethylbenzenes indicate that the fraction of H migration from the α position depended on $K_{cm}$: the fraction increased with increasing $K_{cm}$ (from 0.13 ± 0.01 at $K_{cm}$ = 0.19 eV to 0.24 ± 0.01 at $K_{cm}$ = 0.36 eV) and was likely saturated at ~0.24 at $K_{cm}$ values above 0.28 eV. The value of the isotope effect favoring H migration over D migration (proposed by Leung and Harrison [7]) appeared to be independent of $K_{cm}$. PTR-MS is a powerful tool for investigation of the dependence of branching ratios for proton-transfer reactions with $H_3O^+$ on the mean relative center-of-mass kinetic energies of the reactants.

## References

[1] M.S.B. Munson, F.H. Field, J. Am. Chem. Soc. 88 (1966) 2621.
[2] M.S.B. Munson, F.H. Field, J. Am. Chem. Soc. 89 (1967) 1047.
[3] J.A. Herman, A.G. Harrison, Org. Mass Spectrom. 16 (1981) 423.
[4] D. Kuck, Mass Spectrom. Rev. 9 (1990) 583.

[5] A.G. Harrison, Chemical Ionization Mass Spectrometry, second ed., CRC Press, Boca Raton, FL, 1992.
[6] D. Kuck, Int. J. Mass Spectrom. 213 (2002) 101.
[7] H.-W. Leung, A.G. Harrison, Org. Mass Spectrom. 12 (1977) 582.
[8] H.E. Audier, C. Monteiro, D. Robin, New J. Chem. 13 (1989) 621.
[9] D. Berthomieu, V. Brenner, G. Ohanessian, J.P. Denhez, P. Millié, H.E. Audier, J. Phys. Chem. 99 (1995) 712.
[10] C. Wesdemiotis, H. Scgwarz, C.C. Van de Sande, F.Z. Van Gaever, Naturforsch. B 34 (1979) 495.
[11] NIST Chemistry WebBook, in: W.G. Mallard (Ed.), NIST Standard Reference Database Number 69, National Institute of Standards and Technology, Gaithersburg, MD, 2005 (http://webbook.nist.gov/).
[12] D. Kuck, J. Label. Comp. Radiopharm. 50 (2007) 360.
[13] W. Lindinger, A. Hansel, A. Jordan, Int. J. Mass Spectrom. Ion Processes 173 (1998) 191.
[14] W. Lindinger, A. Hansel, A. Jordan, Chem. Soc. Rev. 27 (1998) 347.
[15] J. de Gouw, C. Warneke, Mass Spectrom. Rev. 26 (2007) 223.
[16] S. Inomata, H. Tanimoto, S. Kameyama, U. Tsunogai, H. Irie, Y. Kanaya, Z. Wang, Atmos. Chem. Phys. 8 (2008) 273.
[17] Y.K. Lau, S. Ikuta, P. Kebarle, J. Am. Chem. Soc. 104 (1982) 1462.
[18] N. Aoki, S. Inomata, H. Tanimoto, Int. J. Mass Spectrom. 263 (2007) 12.
[19] P. Španěl, D. Smith, Int. J. Mass Spectrom. 181 (1998) 1.
[20] A.J. Midey, S. Williams, S.T. Arnold, A.A. Viggiano, J. Phys. Chem. A 106 (2002) 11726.
[21] T. Su, W.J. Chesnavish, J. Chem. Phys. 76 (1982) 5183.
[22] A.A. Viggiano, R.A. Morris, J. Phys. Chem. A 100 (1996) 19227.
[23] K.F. Blom, B. Munson, Anal. Chem. 58 (1986) 2001.
[24] D.R. Hanson, J. Greenberg, B.E. Henry, E. Kosciuch, Int. J. Mass Spectrom. 223–224 (2003) 507.
[25] M.J. Frisch, G.W. Trucks, H.B. Schlegel, G.E. Scuseria, M.A. Robb, J.R. Cheeseman, V.G. Zakrzewski, J.A. Montgomery Jr., R.E. Stratmann, J.C. Burant, S. Dapprich, J.M. Millam, A.D. Daniels, K.N. Kudin, M.C. Strain, O. Farkas, J. Tomasi, V. Barone, M. Cossi, R. Cammi, B. Mennucci, C. Pomelli, C. Adamo, S. Clifford, J. Ochterski, G.A. Petersson, P.Y. Ayala, Q. Cui, K. Morokuma, P. Salvador, J.J. Dannenberg, D.K. Malick, A.D. Rabuck, K. Raghavachari, J.B. Foresman, J. Cioslowski, J. V. Ortiz, A.G. Baboul, B.B. Stefanov, G. Liu, A. Liashenko, P. Piskorz, I. Komaromi, R. Gomperts, R.L. Martin, D.J. Fox, T. Keith, M. A. Al-Laham, C.Y. Peng, A. Nanayakkara, M. Challacombe, P.M. W. Gill, B. Johnson, W. Chen, M.W. Wong, J.L. Andres, C. Gonzalez, M. Head-Gordon, E.S. Replogle, J.A. Pople, Gaussian 98 (Revision A.11), Gaussian, Inc., Pittsburgh, PA, 2001.
[26] M.W. Wong, Chem. Phys. Lett. 256 (1996) 391.
[27] M.W. Chase Jr., J. Phys. Chem. Ref. Data 9 (1998) 1344.